ACS OMEGA

Open Access

http://pubs.acs.org/journal/acsodf

Article

Enantioselective Crystallization on Chiral Hybrid Magnetic Polymeric Particles

Yarden Ben Moshe, Meir Abuaf, Chen Mordechai, Amos Sharoni, and Yitzhak Mastai*

Cite This: *ACS Omega* 2025, 10, 14075−14083

Read Online

ACCESS | Metrics & More | Article Recommendations | Supporting Information

ABSTRACT: A new class of Janus chiral magnetic polymeric particles was fabricated for chiral resolution by enantioselective crystallization. *N*-Acryloyl-L/D-Phe methyl ester beads were prepared with controlled sizes and coated with ferromagnetic permalloy. Chiral discrimination by enantiopure D-Ala crystals was investigated in a model for racemic crystallization. X-ray diffraction and differential scanning calorimetry support the crystallization of the particles. Analysis of optical rotation reveals a D-Ala enantiomeric excess of about 11%, effectively establishing the concept of chiral discrimination by enantioselective crystallization on these Janus chiral magnetic polymeric particles.

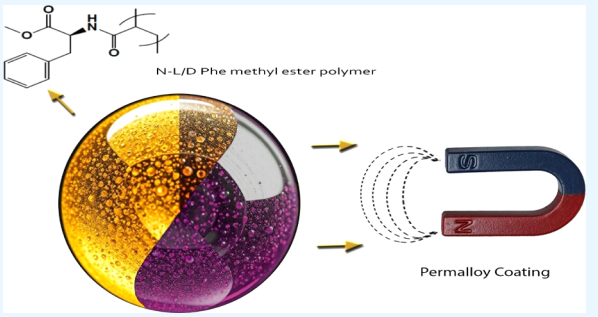

INTRODUCTION

Chiral compound separation has attracted a lot of attention, mainly due to the fact that chirality plays an important role in molecular recognition, which is highly significant in many chemical, biological, and medical applications.[1−3] A chiral molecule may adopt two mirror-image forms, enantiomers, that rotate light in opposite directions. While enantiomers are beneficial for most economic or industrial uses, they may exhibit quite different biological and other behaviors.[4]

The separation of chiral materials is of enormous interest as most bio-organic molecules—proteins, amino acids, sugars, and nucleic acids—are chiral.[5,6] There are currently few ways to prepare optically pure pharmaceuticals; the preferred approach is to resolve racemates with chiral selectors or auxiliaries.[7] Numerous techniques can resolve enantiomers, including selective crystallization,[8] kinetic resolution with enzymes,[9] microbiological techniques,[10] and chiral chromatography.[11−13]

Chiral polymeric micro/nano particles attract great attention owing to their potential application as chiral auxiliaries in resolution by crystallization.[8,14] Various optically active polymers were developed and produced.[15] Three common techniques generate most of these polymers: asymmetric polymerization of prochiral monomers, modification of optically active polymers, and polymerization of optically active monomers.[16] Cölfen et al. demonstrated chiral crystallization by racemate separation with chiral double hydrophilic block copolymers (DHBCs), which are soluble polymers used to achieve racemate separation utilizing crystallization.[17] Chiral DHBCs separated enantiomers in the crystallization of calcium tetrahydrate racemic mixtures as well as in conglomerate systems of sodium ammonium tartrate. Enantioselective crystallization of conglomerate and racemate systems was also demonstrated using chiral polymeric particles based on supersaturated poly-*N*-acrylic amino acids such as phenylalanine, leucine, and alanine in their supersaturated solution. These polymers were tested as initiators of enantioselective crystallization of conglomerate and racemate crystals.[18,19]

Here, aiming to develop particles with different properties, Janus particles (named after the double-faced Roman god)—hybrid particles with two distinct surface properties[20]—were produced for chiral enantioseparation. The bifunctional division of the surface benefits different applications including drug delivery,[20−24] biomedical devices,[25−27] microelectronic components,[25] emulsion stabilizers,[28] water repellents,[29] and stationary phases for chromatography.[13] Three types of Janus particles include soft (polymeric), hybrid (polymeric/inorganic), and hard (inorganic) particles.[25] Polymeric Janus particles have a unique soft behavior owing to their polymer backbone and flexible asymmetric structure.[25] Among composite chiral microparticles, hybrid magnetic/chiral ones are of broad interest owing to their response to magnetic fields.[30,31]

Magnetic separation can easily isolate hybrid particles from enantioselective crystallization and adsorption systems. In addition, a major advantage of magnetic components is their recyclability. Deng and coworkers produced unique hybrid magnetic/chiral microparticles with remarkable optical activity,

Received: December 10, 2024
Revised: February 13, 2025
Accepted: March 10, 2025
Published: April 1, 2025

https://doi.org/10.1021/acsomega.4c11154
ACS Omega 2025, 10, 14075−14083

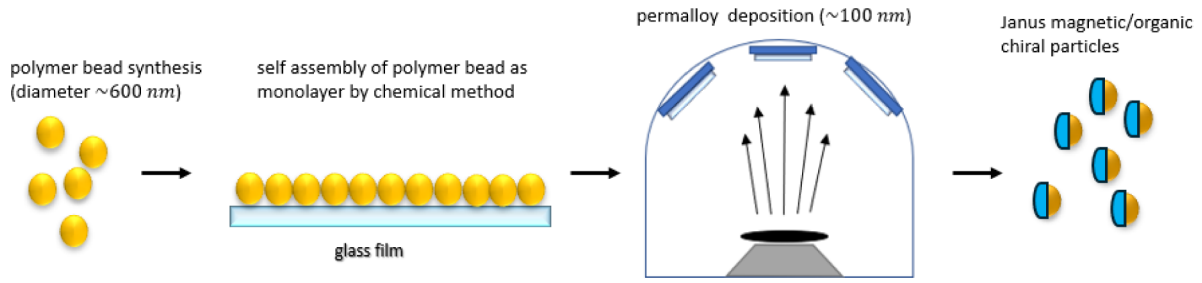

Figure 1. Janus particle fabrication: spherical *N*-acryloyl-L/D-Phe methyl ester beads are diluted in ethanol and drop cast on a glass slide to create a monolayer; the dried slide is inserted into an e-beam for permalloy deposition, and the beads are suspended in solution for future use.

magnetic properties, and recyclability.[30] The hybrid particles can be customized for a variety of applications including chiral sensing, enantiomer resolution, bio-imaging, and asymmetric catalysis.[32−35] Goyal et al. used chiral Fe_3O_4@SiO_2@MP/polymer nanocomposites for the enantiomeric separation of naproxen. The composites were synthesized by copolymerization of acrylamide and ethylene glycol dimethacrylate in the presence of S-naproxen. The magnetic features make this resolution technique a quick and effective procedure.[36]

Here, we present a synthetic method to fabricate Janus (i.e., hybrid) ferromagnetic/chiral microparticles—spherical *N*-acryloyl-L/D-Phe methyl ester beads partially coated with permalloy ($Ni_{80}Fe_{20}$) for chiral separation by enantioselective crystallization on the chiral surface of the particles. Permalloy is known for its high permeability and soft ferromagnetic characteristics,[37,38] which can benefit separation. Figure 1 shows the overall process to fabricate these particles, including dispersion polymerization of *N*-acryloyl-L/D-Phe methyl ester beads, monolayer arrangement of the beads on a glass slide, and permalloy deposition by e-beam evaporation.

Chiral separation via enantioselective crystallization occurs by resolving auxiliaries in the crystallization of enantiomers.[8] We assume that the Janus particles function as selective chiral nuclei during crystallization, reducing the formation energy of one enantiomer and leading to enantioselective crystallization on the chiral hybrid particles. The separation of the enantiomer from the crystallization solution is assisted by the magnetic characteristics.

EXPERIMENTAL SECTION

Chemicals. Analytical-grade chemicals were purchased from Aldrich and used without further purification, including D/L-Phe methyl ester HCl, triethylamine, acryloyl chloride, sodium hydroxide, absolute ethanol absolute, ethyl acetate, *n*-hexane (99%), dichloromethane (DCM), azobis-(isobutyronitrile) (AIBN, 98%), sodium bisulfate, sodium carbonate, sodium chloride, 2-propanol, polyvinylpyrrolidone (PVP, 60 kDa), and magnesium sulfate. Deionized water was purified by passage through an Elastane spectrum reverse osmosis system (Elga, High Wycombe, UK).

Synthesis of Monomers. L/D-Phe methyl ester hydrochloride (20 mmol) was placed in a 250 Liter round-bottom flask. DCM (90 mL) and 2.2 equiv of triethylamine (4.44 g, 6.1 mL) were added, and the mixture was stirred to full dissolution and cooled in an ice bath to 0−5 °C. Acryloyl chloride (1.8 mL, 1.1 equiv) was dissolved in 10 mL of DCM and added dropwise over 1 h while keeping the temperature at 5−10 °C. The mixture was stirred overnight at RT, and the clear DCM solvent was evaporated to dryness, giving a white crude product. EtOAc (100 mL) was added, and after shaking the solution well, the mixture was filtered under vacuum, and the solid (HCl salts) was washed with EtOAc (20 mL). The EtOAc phase was washed with 20 mL of 1 M $NaHSO_4$ (thrice), 5% $NaHCO_3$ and saturated NaCl (twice each), dried with $MgSO_4$, and then filtered. The solvent was removed under vacuum by rotary evaporation to produce the protected L/D-Phe monomer[18,39] (70% yield).

Synthesis of Polymers. In a typical experiment, a solution containing 0.1 g of PVP surfactant, 20 mg of AIBN initiator, 4 mmol of monomer (0.8 g), and 10 mL of solvent (water/2-propanol) in a 20 mL vial was deoxygenated with nitrogen gas. The temperature of the closed shaken vial was preset to 73 °C, and polymerization continued for 24 h before being stopped by cooling to room temperature. The formed insoluble microspheres were separated by centrifugation and washed by extensive centrifugation cycles with water and ethanol. Residual ethanol was removed by extensive centrifugation.[18]

Substrate Preparation. Glass slides precut to 2 × 2 cm^2 were ultrasonically cleaned with acetone and 2-propanol for 5 min, dried with nitrogen, and cleaned further using an RIE process (PICO, Diener Electronic GmbH) with oxygen plasma at a pressure of 0.1 mbar and a power of 150 W for 5 min. Immediately afterward, the slides were covered with hexane and left to dry in a chemical hood. When the hexane fully evaporated, 250 μL of L/D-Phe polymers dispersed in ethanol by sonication at 40 °C (10 mg/7 mL) were drop-cast on the glass and left for at least 24 h (until fully dried).[40,41]

Physical Vapor Deposition. An e-beam evaporator (K. J. Lesker, base pressure 5 × 10^{-7} Torr) was used for deposition.[42−45] The substrate was introduced into the chamber, and the vacuum pressure was reduced to below 1 × 10^{-6} Torr before deposition to avoid outgassing from the polymers during deposition. Permalloy was deposited via an E-beam using a crucible at an evaporation rate of 0.47 Å/*s*. The pressure of the chamber was 3.2 × 10^{-6} Torr, and the deposition thickness was ~100 nm.

Characterization Techniques. NMR spectra were recorded by a Bruker DZH 400/54400 MHz spectrometer (Germany), and FTIR spectroscopy was carried out using a Thermo Scientific Nicolet iS10 FTIR spectrometer (UK) equipped with a Smart iTR attenuated total reflectance sampler containing a single-bounce diamond crystal. DLS measurements were performed using a Zetasizer 3000 HAS (Malvern Instruments Ltd., UK) operating with a 4 mW HeNe laser (632.8 nm), a detector positioned at a scattering angle of 173°, and a temperature-controlled jacket for the cuvette. SEM was performed with an LEO Gemini 1530 Zeiss microscope (Germany) operated at 0.6 kV. Crystallographic structures were analyzed by X-ray diffraction (XRD) measurements using a Bruker AXS D8 Advance diffractometer with Cu Kα

https://doi.org/10.1021/acsomega.4c11154
ACS Omega 2025, 10, 14075−14083

Scheme 1. Synthesis of *N*-Acryloyl-L- or D-Phenylalanine Methyl Ester Monomers

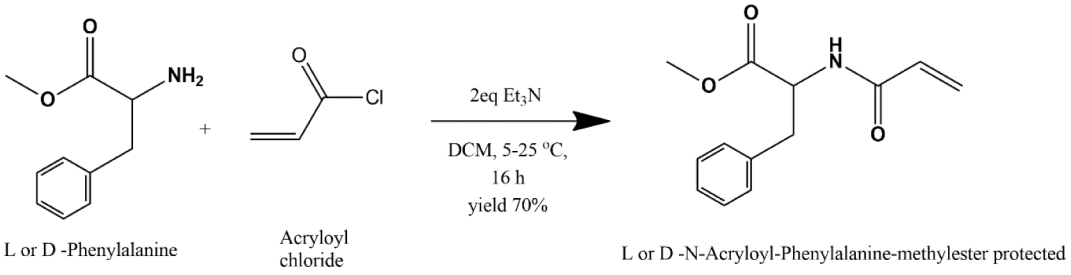

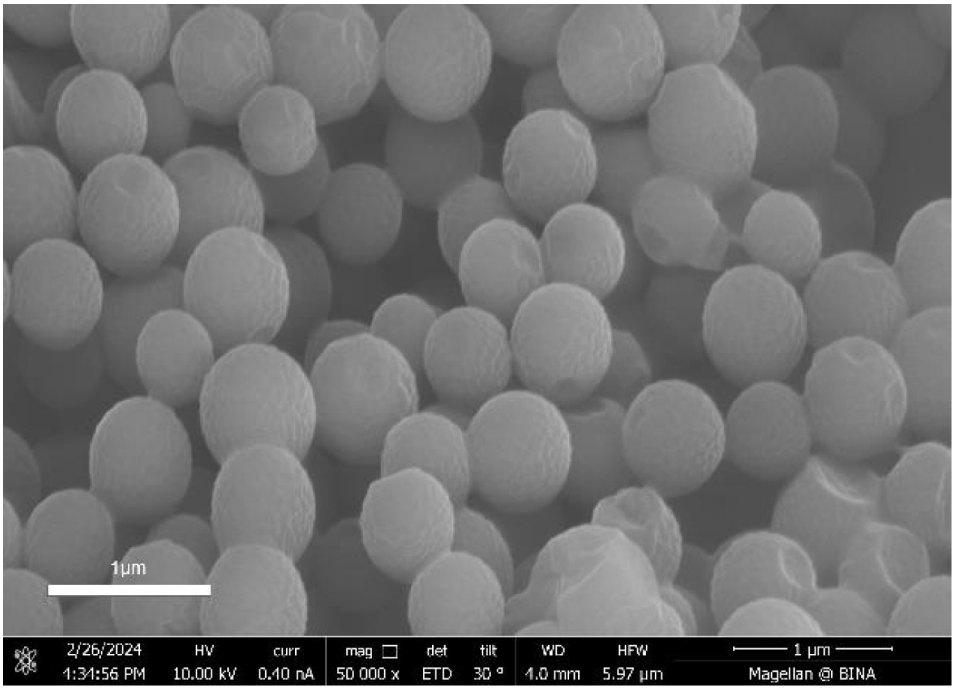

Figure 2. HR-SEM image of poly-D-Phe beads precipitated in 1.2 ratio of water/2-propanol.

radiation (λ = 1.5418 Å), operating at 40 kV/40 mA and collecting data from 2θ = 10° to 80°. Transmission electron microscopy (TEM) images were taken with a JEOL JEM-1400 microscope (UK) operated at 120 kV; samples were prepared by making a dilute suspension of the powders in 2-propanol, placing them dropwise on a 400-mesh carbon-coated copper grid, and vacuum drying the grid. DSC measurements were performed with a Mettler Toledo DSC 822e equipped with a liquid nitrogen cooling accessory and calibrated with indium; samples were heated from 25 to 380 °C at 4 °C/min under N_2 flow. HR-SEM images were taken by using a field-emission FEI Helios 600 instrument. The samples were sputtered with a 3 nm layer of iridium to reduce charging effects.

Selective Chiral adsorption. Adsorption onto the hybrid particle surface was measured by using circular dichroism (CD). Hybrid particles were collected from 13 glass slides (2 × 2 cm^2, ∼20 mg/1 mL). Chiral adsorption was done by incubating the collected particles in 5 mM L/D-Ala solutions at pH 6.5 for 24 h, filtering the solution through a 0.22 μm filter, and measuring the remaining solution using a Chirascan spectrophotometer (Applied Photophysics, UK) at RT. Measurements were carried out in a 1 cm optical path length cell, and the data were recorded from 190−300 nm with a step size and bandwidth of 1 nm. The enantiomeric excess was calculated according to

$$\text{e.e}\ (\%) = \frac{\alpha}{\alpha_{\max}} \times 100$$

where α is measured, and $\alpha_{\max}$ is the maximum specific rotation. The pure L/D-Ala was measured in an aqueous solution as in the adsorption experiments ($\alpha_{\max} = \pm 2.8°$).

Enantioselective Crystallization Experiments. Supersaturated solutions of DL-Ala in deionized water were employed at RT. DL-Ala (9.5 g) was suspended in 50 mL of deionized water, heated to 70 °C, and stirred to complete dissolution. The supersaturated solution was allowed to cool spontaneously to RT and was passed through a 0.22 μm filter. Hybrid particles were collected from 13 glass slides as described above and added to the filtered solution. A shaker was used to continuously move the solution at RT. To monitor the crystallization, 2 mL samples were taken at different times and filtered with a 0.22 μm filter, and the optical rotations of the filtered solutions were measured by a Jasco P-2000 polarimeter using a sodium lamp light source at 589 nm passed through an 8 mm aperture. The enantiomeric excess was calculated according to

$$\text{e.e}\ (\%) = \frac{[R] - [S]}{[R] + [S]} \times 100 = \%R - \%S$$

https://doi.org/10.1021/acsomega.4c11154
ACS Omega 2025, 10, 14075−14083

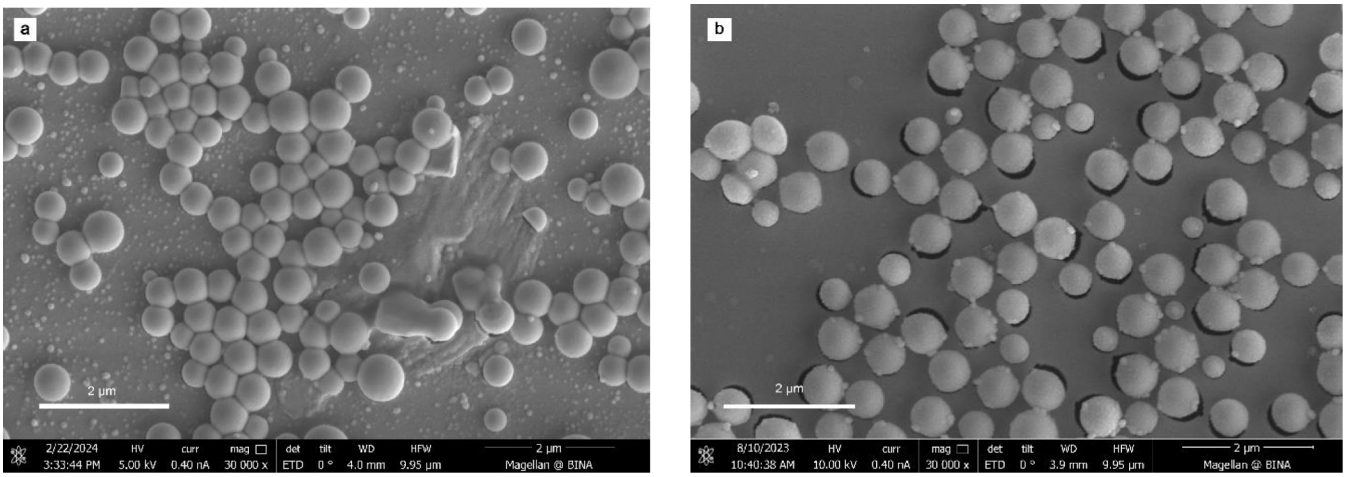

Figure 3. SEM images of poly-L-Phe bead monolayer on a glass slide (a) before and (b) after coating with permalloy (Ni80Fe20).

where e.e (%) is the enantiomeric excess, and $[R]/[S]$ are the concentrations of enantiomers.

RESULTS AND DISCUSSION

N-Acryloyl-L/D-Phe methyl ester beads underwent dispersion polymerization and self-assembly in a monolayer arrangement on a glass slide, and permalloy was deposited on the beads by e-beam evaporation. The chiral selectivity of these hybrid particles was demonstrated with specific model systems of chiral crystallization and adsorption.

Preparation of Magnetic Organic Chiral Particles. *Monomer Synthesis.* Protected L/D-phenylalanine monomer (*N*-acryloyl-L/D-Phe methyl ester) was synthesized in 70% yield (Scheme 1). Monomers were characterized by ^{13}C and ^{1}H nuclear magnetic resonance (NMR), mass spectrometry (MS), and Fourier transform infrared (FTIR) spectroscopy (see Figure S2).

Monomer formation was probed with ^{1}H NMR by recognizing the transformation of a primary amine to a secondary amide: peaks of the amide at δ 6.09 (dd, J = 18, 10 Hz, 1H), terminal ethylene at δ 5.71 (dd, J = 10, 2 Hz, 1H, CH_2), δ 6.02 (brd, J = 8 Hz, 1H, CH_2), and δ 6.29 (dd, J = 18, 2 Hz, 1H, CH), and methyl ester at δ 3.74 (s, 3H). Aromatic peaks are present at δ 7.33−7.19 (m, 3H) and δ 7.14−7.03 (m, 2H).

The FTIR (Figure S5) reveals specific absorption peaks at 3100−3300 and 1650 cm^{-1} corresponding to amide C═O and broad amide N−H stretching bands, as well as peaks at 1750 and 1250 cm^{-1} (ester C═O and stretching bands). Terminal alkene bond stretching ═C−H peaks are observed around 3000 cm^{-1} and aromatic C−H stretching bands appear around 3300 and 2000 cm^{-1} with evident overlap. MS demonstrates base m/z values equivalent to those of phenylalanine (Figure S4).

Polymerization. Microspheres were prepared by the precipitation or dispersion polymerization of poly(*N*-acryloyl-L/D-Phe) in a mixture of water/2-propanol.[30−33] The distribution of polymer diameters is contingent on the water/2-propanol ratio; as this ratio increases, the spheres become larger. Figure 2 presents an SEM image of poly(*N*-acryloyl-D-Phe) particles formed with a water/2-propanol ratio of 1.2. Spherical particles with an average diameter of 600 nm were obtained (±20%, PDI_{DLS} = 0.193) with some roughness on the surface.

Deposition on the Particles. Particle fabrication is demonstrated in Figure 1. For optimal coupling to the poly-D/L-Phe beads, glass slides are treated, and the polymeric beads (∼600 nm with PDI_{DLS} = 0.193) are dispersed in ethanol and drop-cast on the slides to form a monolayer of beads.[22,46,47] After the slides have dried completely, the monolayer is deposited onto polymeric beads using an E-beam evaporator, resulting in Janus particles with a partial permalloy coating. As the polymeric particles are arranged as a monolayer, only their upper side is coated. Finally, the particles are removed from the slide in a solvent (e.g., water or ethanol) under sonication.

Glass slides (2 × 2 cm^2) were precleaned and treated with oxygen plasma to increase the adhesion of the polymeric beads. *n*-Hexane was added dropwise, and the slides were maintained at room temperature (RT) while the hexane was evaporated.[46−48] These procedures enhance the adhesion of the beads to the glass owing to their hydrophobic characteristics. The beads were dispersed in ethanol (10 mg/7 mL) following Indech et al.,[22] and the treated slides were covered with the solution and dried in a chemical hood, resulting in a monolayer of beads. Figure 3a shows the monolayer of poly-L-Phe beads, which is not completely covered. The monolayer on the glass slide provided sufficient protection for the covered portion of each bead's surface. The monolayer was coated with ∼100 nm of permalloy via an e-beam evaporator (Figure 3b). Finally, we removed the particles from the glass slides in a solvent (e.g., water, ethanol) while sonicating. Figure 4 shows SEM and TEM images of the Janus particles after removal from the slide.

Permalloy deposition provides the particles with ferromagnetic features; to examine the magnetic properties, we suspended the particles in water and applied an external magnetic field. We observed the black particles (i.e., coated beads) traveling in the direction of the magnet. Permalloy deposition on the bead monolayer is shown in Figure 3b; the deposition forms a continuous coating layer with a rough texture. Chemical analysis by EDS shows Ni (27%,σ = 0.4) and Fe (5%, σ = 0.2), indicating the presence of permalloy ($Ni_{80}Fe_{20}$) in the particles, as seen in Figure 4. Si, C, N, and O are all present in considerable levels in the organic material. Several impurities can also be seen, such as Na and Ca, in accordance with the carbon tape used for stabilization. The sample was sputtered with a 3 nm layer of iridium to reduce charging effects, and its presence is shown in the EDS spectrum. Figure 5 shows SEM and TEM images after the

https://doi.org/10.1021/acsomega.4c11154
ACS Omega 2025, 10, 14075−14083

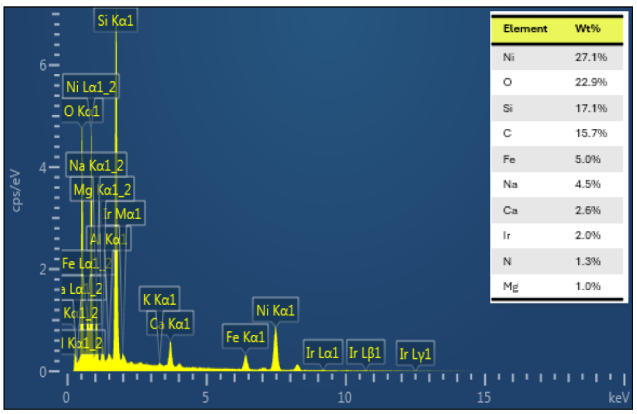

Figure 4. EDS of the monomer after permalloy deposition: Ni 27%, Fe 5%.

removal of the particles from the glass slide; the particles clearly maintained their spherical shape and size and magnetic properties.

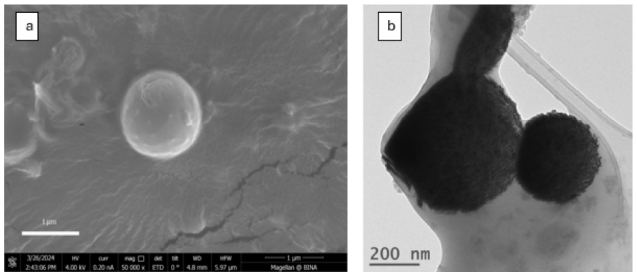

Figure 5. (a) SEM and (b) TEM images of Janus particles removed from the glass slide.

Figure 6 compares the X-ray diffraction (XRD) patterns of the coated and pristine monolayers. The broad groups of peaks around $2\theta = 10°$ and 25° in both samples correspond to the amorphous pattern of glass and polymeric beads. Figure 6b spectrum displays two peaks ($2\theta = 45°$ and 53°), which are not shown in the uncoated spectrum Figure 6a, indicating the presence of permalloy within the particles. Permalloy, crystallized in an FCC structure, includes several crystal planes such as (111), (200), (220), and (311). The peaks at $2\theta = 45°$ and 53° correspond to the (111) and (200) planes, respectively.

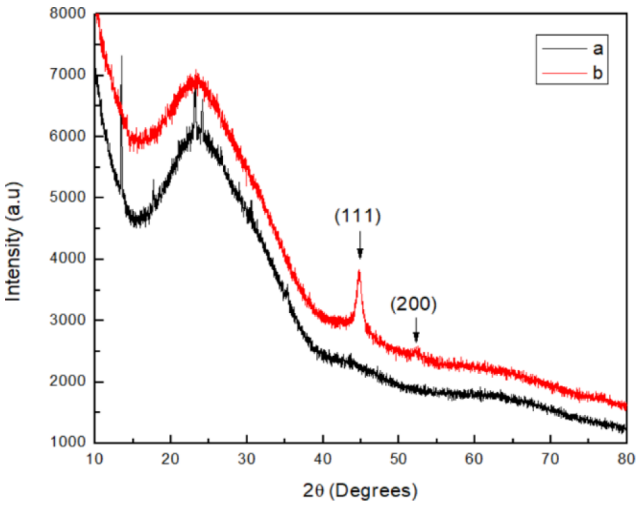

Figure 6. XRD spectra of polymeric bead monolayer on a glass slide (a) without permalloy coating and (b) with permalloy coating.

Chiral Crystallization. To prove the chiral discrimination of the Janus particles, we utilized a select model system of chiral crystallization. In general, three types of chiral molecules crystallize from solution: racemic crystals, which are composed of an equal number of left- and right-handed molecules; conglomerates of individual left- and right-handed crystals of pure enantiomers; and racemic solutions, in which the two enantiomers coexist disorderly within a predetermined concentration range in the crystal lattice. As the enantiomers of a racemic system have the same crystalline structure, their separation is much harder compared to a conglomerate.

We investigated amino acids as a chiral crystallization model system, primarily due to their biological significance and the enormous amount of research on their crystallization and structure. Supersaturated DL-alanine was selected as a model system for studying racemic crystallization under controlled conditions. The stereoselectivity of the hybrid particles is illustrated by the enantioselective crystallization on their surface. Our main theory, supported by previous research on enantioselective crystallization on particles,[8] was that one enantiomer would crystallize onto the particles as they act as enantioselective nuclei.

Time-resolved polarimetry was utilized to monitor the crystallization kinetics and stereoselectivity. In a typical experiment, an optimal amount of DL-Ala is suspended in deionized water. The solution is heated to 70 °C and stirred until the alanine is fully dissolved. Hybrid particles are collected from 13 glass slides (2×2 cm^2) in 2 mL of deionized water by using a sonicator for 5 min. The alanine solution was allowed to cool spontaneously to RT and was combined with the hybrid particle solution for crystallization. After the full crystallization process (1−7 days), the solutions were filtered, and the solid crystals were collected. Figure 7 displays SEM images of the poly-D-Phe-coated spheres after crystallization from the DL-Ala solution. These images demonstrate alanine crystals on the surface of the chiral hybrid particles (Figure 7). Needle-like alanine crystals are shown in Figure 7 in other words, the spherical chiral hybrid particles are filled with crystals on their surface and in the solution.

To examine enantioselective crystallization on the chiral hybrid particles, we utilized powder XRD and differential scanning calorimetry (DSC). Here, we should demonstrate that the crystals produced in this series of experiments are more like enantiomers than to the racemic state due to their properties.[49] For instance, as the enantiomers' crystalline structures differ from those of the corresponding racemic compound, their XRD patterns are distinct.[50]

In addition, as racemates and pure enantiomers differ in thermal behavior, traces of enantiomers can be investigated by DSC.[50] The XRD pattern of the collected crystals shows no difference from that of the racemic DL-Ala powder. The solid samples were examined by DSC, which provided chiral information about the crystals. A small number of pure enantiomers lower the melting point of the racemates in racemic compounds. The DSC curves of pure DL-Ala crystals and the chiral hybrid particles are shown in Figure 8. Pure racemic DL-Ala shows a melting peak at 283 °C, while the DSC analysis of DL-Ala crystals crystallized onto chiral hybrid particles or crystals without particles shows a shift of the

https://doi.org/10.1021/acsomega.4c11154
ACS Omega 2025, 10, 14075−14083

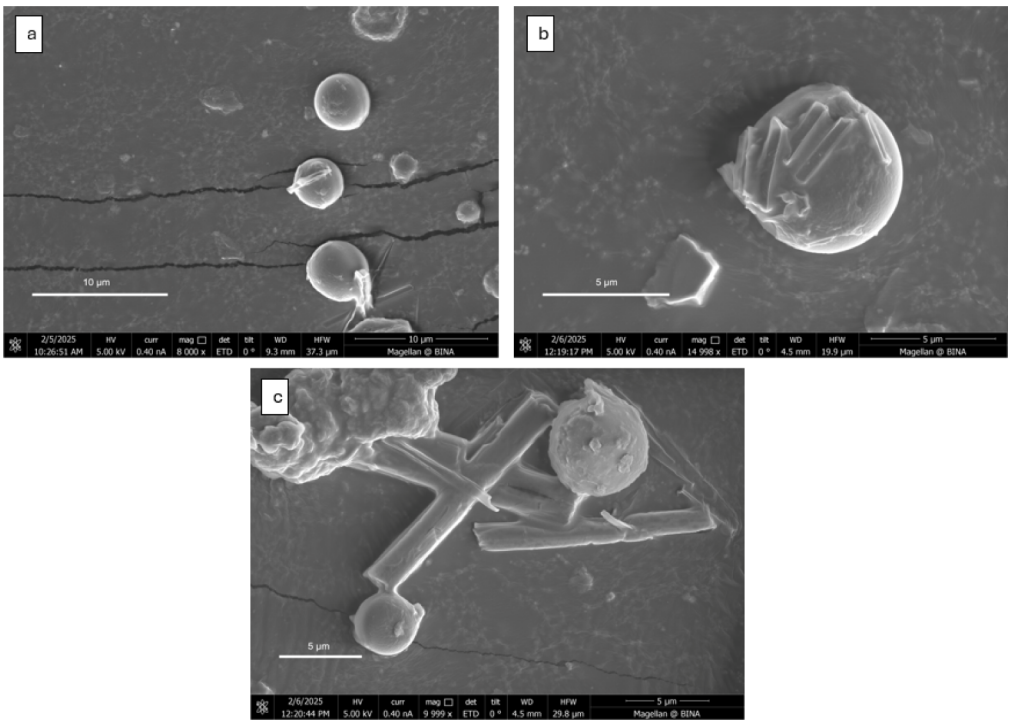

Figure 7. (a−c) HR-SEM images of poly-D-Phe coated spheres after crystallization from DL-Ala solution.

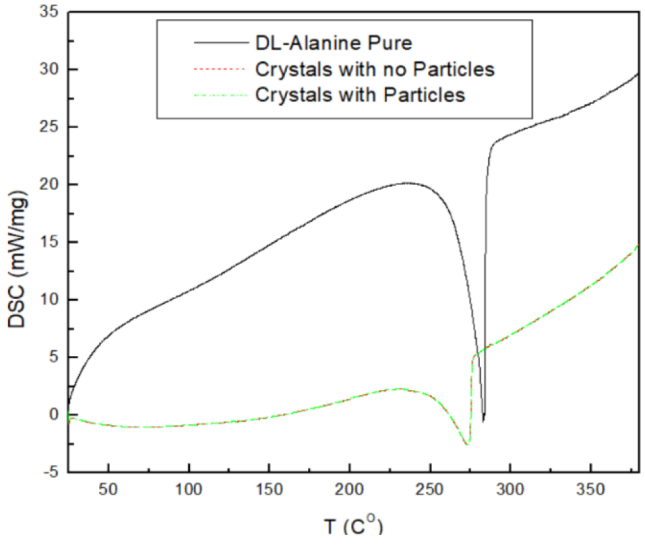

Figure 8. DSC of DL-Ala crystals: pure (black) and crystallized with no particles (red) or on the chiral hybrid particles (green).

melting peak to 273 °C. This shift in the melting point of the crystals indicates the presence of pure enantiomeric alanine crystals.

The above characterization techniques, SEM and DSC, clearly demonstrate enantioselective crystallization onto the chiral hybrid particles. However, it is tough to learn quantitative information about chiral separation based only on these techniques. Time-dependent optical rotation experiments were performed throughout the crystallization process to measure the chiral efficiency of the particles.

The experiment was performed as follows: approximately 20 mg of hybrid particles was added to a supersaturated DL-Ala solution at RT. A 2 mL sample was taken out of the crystallization solution every hour for 4 h to track its optical activity over time. Two other samples were taken after 24 and 72 h. Each sample was filtered with a 0.22 μm filter to obtain a clear solution; optical rotations were measured in a polarimeter cell with a 1 cm path length with an accuracy of $\alpha = \pm 0.05°$. Figure 9 displays data from one of these experiments. Analyses of the optical activity spectra confirm chiral discrimination on the chiral hybrid particles during crystallization.

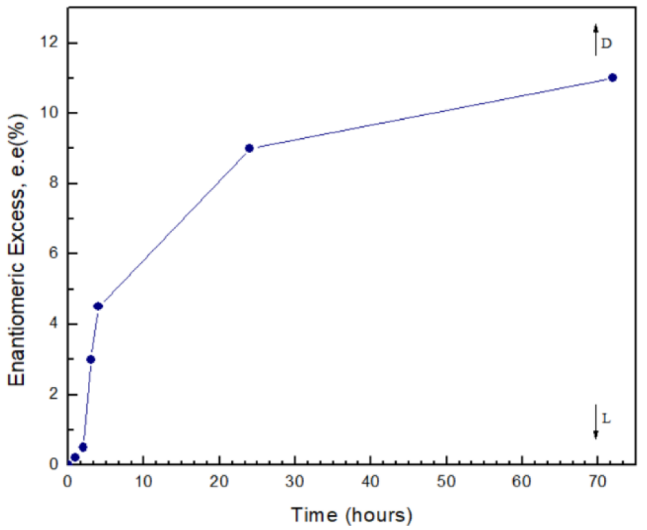

Figure 9. Time-resolved polarimetry for DL-Ala crystallization with poly-D-Phe coated spheres.

At the early stages of crystallization, an enantiomeric excess of approximately 5% was measured, which increased over time and reached 11% at the end of the process. By examination of the optical activity of the crystallization solution, a significant excess of the D-enantiomer revealed that the solid phase is enriched with L-Ala. Analogous experiments measured the

https://doi.org/10.1021/acsomega.4c11154
ACS Omega 2025, 10, 14075−14083

optical activity of the crystals obtained from the chiral hybrid particles. Crystals (1 mg/5 mL) were collected and dissolved in 0.1 M HCl. The optical activity was not clear, as difficulties were encountered with the separation of the formed crystals. Crystallization experiments as described above with poly-L-Phe-coated spheres achieved an L-enantiomeric excess of approximately 5% after 24 h of crystallization.

Chiral adsorption measurements were conducted to prove the stereoselective adsorption of L/D-Ala on the chiral surface of the hybrid particles. Chiral adsorption was performed by incubating 20 mg/mL of hybrid particles in a 5 mM L/D-Ala solution at pH 6.5 for 24 h, passing the solution through a 0.22 μm filter, and measuring the remaining solution with a spectrophotometer at RT (Figure 10). We used a sonicator bath to wash the particles with water in order to cycle them between adsorption studies.

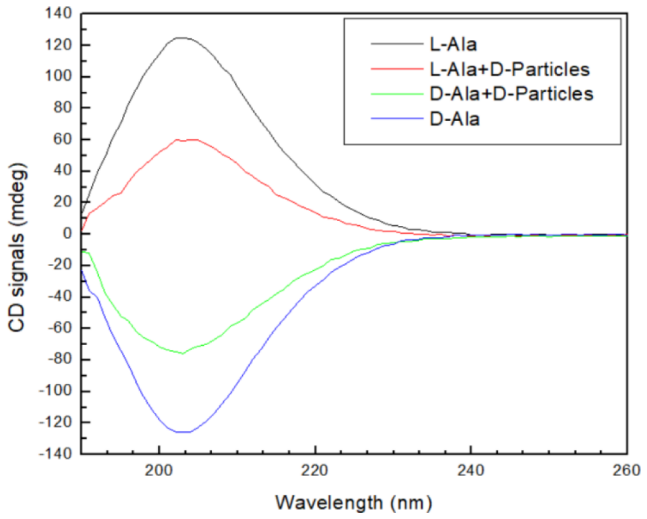

Figure 10. Selective adsorbance of L/D-Ala onto poly-D-Phe coated spheres. CD spectra of 5 mM L/D-Ala pure (blue and black) were incubated with poly-D-Phe coated particles for 24 h (red and green).

Figure 10 displays a significant difference in alanine adsorption to hybrid particles. The poly-D-Phe coated particles recognized and adsorbed better to L-Ala. The hybrid particles adsorbed 52% of L-alanine compared to 41% of D-alanine during the incubation period. Based on equilibrium concentrations for L/D enantiomers, we found 10% discrimination of enantioselectivity. Although not very high compared to other chiral materials,[13] it is important to consider this figure in a larger context. In chiral chromatography, a relative retention (R) factor of 1.5 is sufficient to obtain successful enantiomeric separation. Chiral adsorption is an additional technique that provides an indication of the chiral behavior of the particle surfaces.

In addition, we examine the effect of the permalloy coating on the CD signal of these particles (see Figure S6). We measured 5 mg/mL of D-Phe spheres in water before and after permalloy coating. The CD spectra show that the permalloy coating reduces the CD signal. We assume that the permalloy covering is shielding the light interaction of the particles.

In conclusion, our results clearly demonstrate that chiral hybrid particles are subject to chiral discrimination and enantioselective crystallization. Based on chiral recognition and nucleation/crystallization theory, the mechanism for enantioselective crystallization seen on the surface of the chiral hybrid particles can be described. Our study indicates that crystal nucleation and growth on chiral hybrid particles start at their surface. Chiral adsorption measurements indicate that these chiral spheres have strong molecular recognition of the L-enantiomers.

CONCLUSIONS

Enantioselective crystallization is expected to remain a crucial and profitable procedure for the industrial synthesis of enantiomers. Here, spherical chiral Janus polymeric particles with magnetic characteristics were prepared and used to resolve optically active isomers. Chiral Janus polymeric particles based on *N*-acryloyl-L/D-Phe methyl ester beads with a permalloy coating show ferromagnetic properties, which were utilized for efficient chiral resolution. The spherical hybrid particles have a narrow size distribution, which can be controlled by varying the synthesis conditions.

The chiral discrimination of the Janus chiral magnetic spheres was investigated for DL-Ala crystallization as a model system for racemic crystals. SEM and DSC indicate the crystallization of enantiopure crystals on the chiral surface of these particles. Optical rotation measurements demonstrate an enantiomeric excess of ca. 11%. Although this figure is not particularly high, the basic concept of chiral discrimination by enantioselective crystallization on chiral hybrid spheres is demonstrated.

Permalloy, deposited on these particles, is known for its high permeability and soft ferromagnetic characteristics. Further study of these properties can optimize chiral separation. Overall, our methods demonstrate the general idea of molecular recognition at chiral surfaces. Furthermore, enantioselective crystallization employing chiral particles can be effectively combined with current technologies to produce better chiral resolution.

Subsequent research utilizing chiral functions and tailored polymer morphology may yield notable enhancements in enantiomeric excess. The enantioselective crystallization on hybrid particles may be optimized by further studies of the polymeric component (i.e., using several types of *N*-acryloyl-amino acid beads) or by varying crystallization conditions such as temperature and supersaturation level.

New chiral resolution techniques can be developed by producing Janus chiral magnetic polymeric spheres in a range of sizes, morphologies, and chemical functions. In addition, the magnetic/chiral particles can allow a variety of applications besides enantiomeric resolution, including chiral sensing, bioimaging, and asymmetric catalysis. We believe that employing Janus chiral magnetic polymeric spheres as chiral resolving auxiliaries will help clarify chiral recognition on polymeric surfaces and offer more knowledge of chiral discrimination throughout the crystallization process.

ASSOCIATED CONTENT

Supporting Information

The Supporting Information is available free of charge at https://pubs.acs.org/doi/10.1021/acsomega.4c11154.

Scheme of *N*-acryloyl-L/D-Phe methyl ester polymerization (Figure S1); table of ^{1}H, ^{13}C NMR, and MS characterization of the *N*-acryloyl-L/D-Phe monomers (Figure S2); ^{13C} and ^{1}H NMR spectra of the *N*-acryloyl-L/D-Phe methyl ester monomers (Figure S3); mass spectrum of the monomers (Figure S4); FTIR

https://doi.org/10.1021/acsomega.4c11154
ACS Omega 2025, 10, 14075−14083

absorbance spectrum of the *N*-acryloyl-L-Phe methyl ester monomers (Figure S5); CD spectra of 5 mM D-Phe beads in water before and after permalloy coating: (a) D-Phe beads before coating and (b) D-Phe beads after the coating (Figure S6); FTIR absorbance spectra of D-Phe hybrid particles (a) before D-Ala crystallization on the particles and (b) after D-Ala crystallization on the particles (Figure S7); HR-TEM diffraction pattern of the chiral hybrid particles which correspond to (111) and (200) planes (Figure S8) (PDF)

AUTHOR INFORMATION

Corresponding Author

Yitzhak Mastai − *Department of Chemistry, Bar-Ilan University, Ramat Gan 5900002, Israel; Bar-Ilan Institute of Nanotechnology and Advanced Materials (BINA), Bar-Ilan University, Ramat Gan 5900002, Israel;* orcid.org/0000-0002-7330-0886; Email: mastai@mail.biu.ac.il

Authors

Yarden Ben Moshe − *Department of Chemistry, Bar-Ilan University, Ramat Gan 5900002, Israel; Bar-Ilan Institute of Nanotechnology and Advanced Materials (BINA), Bar-Ilan University, Ramat Gan 5900002, Israel*

Meir Abuaf − *Department of Chemistry, Bar-Ilan University, Ramat Gan 5900002, Israel; Bar-Ilan Institute of Nanotechnology and Advanced Materials (BINA), Bar-Ilan University, Ramat Gan 5900002, Israel*

Chen Mordechai − *Department of Physics, Bar-Ilan University, Ramat Gan 5900002, Israel; Bar-Ilan Institute of Nanotechnology and Advanced Materials (BINA), Bar-Ilan University, Ramat Gan 5900002, Israel*

Amos Sharoni − *Department of Physics, Bar-Ilan University, Ramat Gan 5900002, Israel; Bar-Ilan Institute of Nanotechnology and Advanced Materials (BINA), Bar-Ilan University, Ramat Gan 5900002, Israel;* orcid.org/0000-0003-3659-0818

Complete contact information is available at: https://pubs.acs.org/10.1021/acsomega.4c11154

Funding

This research was supported by the Israel Science Foundation (ISF Grant #2546/21).

Notes

The authors declare no competing financial interest.

ACKNOWLEDGMENTS

Y.B.M. thanks the Bar-Ilan President scholarship program for Ph.D.

REFERENCES

(1) Barron, L. D. Symmetry and Molecular Chirality. *Chem. Soc. Rev.* **1986**, *15* (2), 189−223.

(2) Prelog, V. Chirality in Chemistry. *Science* **1976**, *193* (4247), 17−24.

(3) Barron, L. D. Chirality and Life. *Space Sci. Rev.* **2008**, *135* (1−4), 187−201.

(4) Amabilino, D. B. Chirality at the Nanoscale. Nanoparticles, Surfaces, Materials and more. Edited by David B. Amabilino. *Angew. Chem., Int. Ed.* **2010**, *49* (8), 1355.

(5) Ayon, N. J. Features, Roles and Chiral Analyses of Proteinogenic Amino Acids. *AIMS Molecular Science* **2020**, *7* (3), 229−268.

(6) Martínez, R. F.; Cuccia, L. A.; Viedma, C.; Cintas, P. *On the Origin of Sugar Handedness: Facts, Hypotheses and Missing Links-A Review*; Springer: Netherlands, 2022; Vol. *52*.

(7) Wainer, I. W. *Drug Stereochemistry, Analytical Methods and Pharmacology*, 2nd ed.; Marcel Dekker: New York, 1993.

(8) Medina, D. D.; Mastai, Y. Chiral Polymers and Polymeric Particles for Enantioselective Crystallization. *Isr. J. Chem.* **2018**, *58* (12), 1330−1337.

(9) Kamal, A.; Azhar, M. A.; Krishnaji, T.; Malik, M. S.; Azeeza, S. Approaches Based on Enzyme Mediated Kinetic to Dynamic Kinetic Resolutions: A Versatile Route for Chiral Intermediates. *Coord. Chem. Rev.* **2008**, *252* (5−7), 569−592.

(10) Allenmark, S.; Bomgren, B.; Borén, H. Enantioselective Microbial Degradation of Some Racemates Studied by Chiral Liquid Chromatography. *Enzyme Microb. Technol.* **1986**, *8* (7), 404−408.

(11) Chankvetadze, B. *Enantioseparations By High-Performance Liquid Chromatography Using Polysaccharide-Based Chiral Stationary Phases: An Overview. Methods Mol Bio.* **2013**, *970*, 81−111.

(12) Chankvetadze, B.; Kartozia, I.; Yamamoto, C.; Okamoto, Y. Comparative Enantioseparation of Selected Chiral Drugs on Four Different Polysaccharide-Type Chiral Stationary Phases Using Polar Organic Mobile Phases. *J. Pharm. Biomed. Anal.* **2002**, *27* (3−4), 467−478.

(13) Subramanian, G*Chiral Separation Techniques: A Practical Approach*. Wiley; 2007. 641

(14) Wang, D.; Sang, J.; Wang, Y.; Zhang, B.; Liu, Z.; Han, D.; Gong, J. Crystallization Resolution of Racemic Compounds via Chiral Surfactant. *Chem. Eng. Sci.* **2024**, *299* (May), 120540.

(15) Alzubi, M.; Arias, S.; Rodríguez, R.; Quiñoá, E.; Riguera, R.; Freire, F. Chiral Conflict as a Method to Create Stimuli-Responsive Materials Based on Dynamic Helical Polymers. *Angew. Chem., Int. Ed.* **2019**, *131* (38), 13499−13503.

(16) Yamamoto, C.; Okamoto, Y. Optically Active Polymers for Chiral Separation. *Bull. Chem. Soc. Jpn.* **2004**, *77* (2), 227−257.

(17) Mastai, Y.; Sedlak, M.; Ĉlfen, H.; Antonietti, M. The Separation of Racemic Crystals into Enantiomers by Chiral Block Copolymers. *Chem. Eur. J.* **2002**, *8* (11), 2429.

(18) Abuaf, M.; Mastai, Y. Synthesis of Multi Amino Acid Chiral Polymeric Microparticles for Enantioselective Chemistry. *Macromol. Chem. Phys.* **2020**, *221* (24), 2000328.

(19) Menahem, T.; Mastai, Y. Chiral Soluble Polymers and Microspheres for Enantioselective Crystallization. *J. Polym. Sci., Part A: Polym. Chem.* **2006**, *44* (9), 3009−3017.

(20) Sundararajan, P.; Wang, J.; Rosen, L. A.; Procopio, A.; Rosenberg, K. Engineering Polymeric Janus Particles for Drug Delivery Using Microfluidic Solvent Dissolution Approach. *Chem. Eng. Sci.* **2018**, *178*, 199−210.

(21) Yamala, A. K.; Nadella, V.; Mastai, Y.; Prakash, H.; Paik, P. Poly- N -Acryloyl-(l -Phenylalanine Methyl Ester) Hollow Core Nanocapsules Facilitate Sustained Delivery of Immunomodulatory Drugs and Exhibit Adjuvant Properties. *Nanoscale* **2017**, *9* (37), 14006−14014.

(22) Indech, G.; Geri, L.; Mordechai, C.; Ben Moshe, Y.; Mastai, Y.; Shefi, O.; Sharoni, A. Controlled Synthesis of Multifunctional Dome-Shaped Micro- and Nano-Structures via a Robust Physical Route for Biological Applications. *J. Mater. Chem. B* **2023**, *11* (30), 7094−7102.

(23) Peres, L. B.; Preiss, L. C.; Wagner, M.; Wurm, F. R.; De Araújo, P. H. H.; Landfester, K.; Muñoz-Espí, R.; Sayer, C. ALTMET Polymerization of Amino Acid-Based Monomers Targeting Controlled Drug Release. *Macromolecules* **2016**, *49* (18), 6723−6730.

(24) Ding, H. M.; Ma, Y. Q. Interactions between Janus Particles and Membranes. *Nanoscale* **2012**, *4* (4), 1116−1122.

(25) Fan, X.; Yang, J.; Loh, X. J.; Li, Z. Polymeric Janus Nanoparticles: Recent Advances in Synthetic Strategies, Materials Properties, and Applications. *Macromol. Rapid Commun.* **2019**, *40* (5), 1800203.

(26) Le, T. C.; Zhai, J.; Chiu, W. H.; Tran, P. A.; Tran, N. Janus Particles: Recent Advances in the Biomedical Applications. *Int. J. Nanomed* **2019**, *14*, 6749−6777.

(27) Gao, Y.; Yu, Y. How Half-Coated Janus Particles Enter Cells. *J. Am. Chem. Soc.* **2013**, *135* (51), 19091−19094.
(28) Lone, S.; Cheong, I. W. Fabrication of Polymeric Janus Particles by Droplet Microfluidics. *RSC Adv.* **2014**, *4* (26), 13322−13333.
(29) Pan, D.; Mou, F.; Li, X.; Deng, Z.; Sun, J.; Xu, L.; Guan, J. Multifunctional Magnetic Oleic Acid-Coated MnFe2O4/Polystyrene Janus Particles for Water Treatment. *J. Mater. Chem. A* **2016**, *4* (30), 11768−11774.
(30) Zhang, H.; Qian, G.; Song, J.; Deng, J. Optically Active, Magnetic Microparticles: Constructed by Chiral Helical Substituted Polyacetylene/Fe3O4 Nanoparticles and Recycled for Uses in Enantioselective Crystallization. *Ind. Eng. Chem. Res.* **2014**, *53* (44), 17394−17402.
(31) Zhong, H.; Zhao, B.; Deng, J. Chiral Magnetic Hybrid Materials Constructed from Macromolecules and Their Chiral Applications. *Nanoscale* **2021**, *13* (27), 11765−11780.
(32) Liu, Y.; Li, Z.; Jia, L. Synthesis of Molecularly Imprinted Polymer Modified Magnetic Particles for Chiral Separation of Tryptophan Enantiomers in Aqueous Medium. *J. Chromatogr. A* **2020**, *1622*, 461147.
(33) Liu, D.; Zhang, L.; Li, M.; Yang, W.; Deng, J. Magnetic Fe 3O 4-PS-Polyacetylene Composite Microspheres Showing Chirality Derived from Helical Substituted Polyacetylene. *Macromol. Rapid Commun.* **2012**, *33* (8), 672−677.
(34) Gijs, M. A. M.; Lacharme, F.; Lehmann, U. Microfluidic Applications of Magnetic Particles for Biological Analysis and Catalysis. *Chem. Rev.* **2010**, *110* (3), 1518−1563.
(35) Lin, Y. -L.; Chu, J. -H.; Lu, H. -J.; Liu, N.; Wu, Z. -Q. Facile Synthesis of Optically Active and Magnetic Nanoparticles Carrying Helical Poly(Phenyl Isocyanide) Arms and Their Application in Enantioselective Crystallization. *Macromol. Rapid Commun.* **2018**, *39* (5), 1700685.
(36) Goyal, G.; Bhakta, S.; Mishra, P. Surface Molecularly Imprinted Biomimetic Magnetic Nanoparticles for Enantioseparation. *ACS Appl. Nano Mater.* **2019**, *2* (10), 6747−6756.
(37) Yousefi, E.; Sharafi, S.; Irannejad, A. The Structural, Magnetic, and Tribological Properties of Nanocrystalline Fe-Ni Permalloy and Fe-Ni-TiO2 Composite Coatings Produced by Pulse Electro Co-Deposition. *J. Alloys Compd.* **2018**, *753*, 308−319.
(38) Sun, Y.; Zhang, J.; Zong, Y.; Deng, X.; Zhao, H.; Feng, J.; He, M.; Li, X.; Peng, Y.; Zheng, X. Crystalline-Amorphous Permalloy@ Iron Oxide Core-Shell Nanoparticles Decorated on Graphene as High-Efficiency, Lightweight, and Hydrophobic Microwave Absorbents. *ACS Appl. Mater. Interfaces* **2019**, *11* (6), 6374−6383.
(39) Abuaf, M.; Das, S.; Mastai, Y. Organocatalytic Chiral Polymeric Nanoparticles for Asymmetric Aldol Reaction. *RSC Adv.* **2023**, *13* (3), 1580−1586.
(40) Indech, G.; Geri, L.; Mordechai, C.; Ben Moshe, Y.; Mastai, Y.; Shefi, O.; Sharoni, A. Controlled synthesis of multifunctional dome-shaped micro- and nano-structures via a robust physical route for biological applications. *J. Mater. Chem. B* **2023**, *11* (30), 7094−7102.
(41) Souheng, W. U. *Polymer Interface and Adhesion*; Taylor & Francis Group, 1982; Vol. *4*.
(42) Bentolila, A.; Vlodavsky, I.; Ishai-Michaeli, R.; Kovalchuk, O.; Haloun, C.; Domb, A. J. Poly(N-Acryl Amino Acids): A New Class of Biologically Active Polyanions. *J. Med. Chem.* **2000**, *43* (13), 2591−2600.
(43) Bentolila, A.; Vlodavsky, I.; Haloun, C.; Domb, A. J. Synthesis and Heparin-like Biological Activity of Amino Acid-Based Polymers. *Polym. Adv. Technol.* **2000**, *11* (8−12), 377−387.
(44) Muñoz-Espí, R.; Mastai, Y.; Gross, S.; Landfester, K. Colloidal Systems for Crystallization Processes from Liquid Phase. *CrystEngcomm* **2013**, *15* (12), 2175−2191.
(45) Boyer, C.; Liu, J.; Wong, L.; Tippett, M.; Bulmus, V.; Davis, T. P. Stability and Utility of Pyridyl Disulfide Functionality in RAFT and Conventional Radical Polymerizations. *J. Polym. Sci., Part A: polym. Chem* **2008**, *46* (21), 7207−7224.
(46) Hu, L.; Chen, M.; Fang, X.; Wu, L. Oil−Water Interfacial Self-Assembly: A Novel Strategy for Nanofilm and Nanodevice Fabrication. *Chem. Soc. Rev.* **2012**, *41* (3), 1350−1362.
(47) Goldenberg, L. M.; Wagner, J.; Stumpe, J.; Paulke, B. R.; Görnitz, E. Simple Method for the Preparation of Colloidal Particle Monolayers at the Water/Alkane Interface. *Langmuir* **2002**, *18* (14), 5627−5629.
(48) Park, Y. K.; Yoo, S. H.; Park, S. Assembly of Highly Ordered Nanoparticle Monolayers at a Water/ Hexane Interface. *Langmuir* **2007**, *23* (21), 10505−10510.
(49) Li, Z. J.; Zell, M. T.; Munson, E. J.; Grant, D. J. W. Characterization of Racemic Species of Chiral Drugs Using Thermal Analysis, Thermodynamic Calculation, and Structural Studies. *J. Pharm. Sci.* **1999**, *88* (3), 337−346.
(50) Eliel, E. L.; Wilen, S. H.; Mander, L. N.*Stereochemistry Of Organic Compounds*John Wiley & Sons19941267

https://doi.org/10.1021/acsomega.4c11154
ACS Omega 2025, 10, 14075−14083